Heliyon 9 (2023) e19295

Contents lists available at ScienceDirect

Heliyon

journal homepage: www.cell.com/heliyon

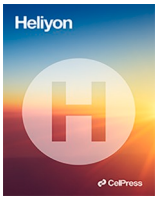

Synthesis, characterization, and antiparasitic effects of zinc oxide nanoparticles-eugenol nanosuspension against *Toxoplasma gondii* infection

Kourosh Cheraghipour [a], Amal Khudair Khalaf [b], Kobra Moradpour [a], Masoomeh Zivdari [a], Marjan Beiranvand [a], Pegah Shakib [a], Hossein Mahmoudvand [c,*], Abdolrazagh Marzban [a,**]

[a] *Razi Herbal Medicines Research Center, Lorestan University of Medical Sciences, Khorramabad, Iran*
[b] *Department of Microbiology, College of Medicine, University of Thiqar, Iraq*
[c] *Hepatitis Research Center, Lorestan University of Medical Sciences, Khorramabad, Iran*

ARTICLE INFO

Keywords:
Zinc oxid nanoparticles
Eugenol
ZnO@Eug NSus
Toxoplasma gondii
Antiparasitic activity

ABSTRACT

Background: In this study, zinc oxide nanoparticles-coated with eugenol (ZnO@Eug) were synthesized and evaluated as a nanosuspension (NSus) formulation against *Toxoplasma gondii* in vitro and in vivo.
Methods: An anti-*Toxoplasma* activity assay for ZnO@Eug NSus was conducted in vitro, ex vivo, and in vivo. FTIR spectroscopy confirmed the formation of ZnO@Eug NSus by detecting several functional groups involved; EDX and SEM demonstrated the grain of ZnO-NPs embedded with Eug and compositional purity.
Results: Surface charge (ZP) and size distribution (DLS) of ZnO@Eug NSus were determined to be −22.7 mV and 109.6 nm, respectively. According to the release kinetics, approximately 60% of the ZnO-NPs and Eug were released in the first 45 min. In the cytotoxicity assay, ZnO-NPs, Eug, and ZnO@Eug NSus had IC_{50} values of 71.85, 22.39, and 2.02 mg/mL, respectively. The therapeutic efficacy of ZnO@Eug against *T. gondii* was 56.3%, which was not significantly different from that of spiramycin (58.9%) (Positive-control). The tissue tachyzoites in the liver, spleen, and peritoneum were less than 50% in groups treated with Eug, spiramycin, and ZnO@Eug NSus compared to the control. ZnO@Eug-treated groups showed a survival rate of up to 13 days.
Conclusions: The ZnO@Eug NSus demonstrated antiparasitic activity against *T. gondii* with minimal toxic effects and high efficiency in increasing the survival of infected mice. The nanoformulations of ZnO-NPs incorporated with Eug could, in the future, be considered for treating toxoplasmosis in humans and animals if a detailed study was conducted to determine the precise dose and measure side effects.

Abbreviations: ZnO@Eug, Zinc oxide nanoparticles-coated with eugenol; ZP, surface charge; DLS, size distribution; PVA, Polyvinyl alcohol; DMSO, dimethyl sulfoxide; ANOVA, One-way analysis of variance (ANOVA).

* Corresponding author.
** Corresponding author.
E-mail addresses: dmahmodvand@gmail.com (H. Mahmoudvand), marzbn@gmail.com (A. Marzban).

https://doi.org/10.1016/j.heliyon.2023.e19295
Received 22 April 2023; Received in revised form 4 August 2023; Accepted 17 August 2023
Available online 19 August 2023

1. Introduction

Toxoplasma gondii is a protozoan parasite of the Apicomplexia phylum that causes disease in humans and other warm-blooded animals. The parasite can be spread to humans through foods, groundwater, soil, and vegetables that have been infected with it [1]. Infection with *Toxoplasma* is primarily caused by cats' shedding of parasitic oocysts. Immune responses play an important role in disease severity. Therefore, patients with weakened immune systems may be at risk of developing the fatal form of the disease [2]. In many cases, *Toxoplasma* can remain latent in the brain and muscles of people for a long time [3]. One of the most serious diseases that can occur during pregnancy is the transmission of *Toxoplasma* to the fetus [4]. Toxoplasmosis is typically treated with dihydrofolate reductase (DHFR) inhibitors, such as pyrimethamine (PYR). Although these drugs were effective against the active Tachyzoites form of *Toxoplasma*, they could not inhibit the Bradyzoites and Sporozoites forms [5]. Thus, a combination of trimethoprim and sulfamethoxazole may be recommended to treat *T. gondii* infections. Among the serious challenges in combination therapy are complications related to the suppression of bone marrow and the impairment of the renal system [6]. Consequently, finding new therapeutic strategies with minimal side effects is the foremost priority in the fight against toxoplasmosis. Using herbal metabolites has become a valuable alternative to many conventional drugs for treating infectious diseases. However, studies show that plant metabolites have limitations, including low bioavailability, physiological instability, and potential toxic properties [7].

Eug is one of the volatile natural terpenoids (allylbenzene) that is the major part of the essential oil in *Syzygium aromaticum*. So far, several studies have been conducted on the biological activities of Eug, such as antibacterial, antifungal, anticancer, antioxidant, anti-inflammatory, and antiparasitic [1–8]. Eug has been recognized as an edible and safe substance for human food consumption [9,10].

Nanomedicine refers to using nanomaterials to diagnose, treat, and prevent diseases in humans and animals. In recent years, scientists have been focusing on ways to produce more biomedically suitable nanomaterials with environmentally friendly processes. ZnO-NPs are inorganic nanostructures with multiple advantages over metal NPs. ZnO-NPs have superior optical, semiconductivity, and piezoelectric properties, making them useful in various fields, including cosmetics, catalysis, energy storage, electronics, textiles, and health. Furthermore, ZnO-NPs exhibit a variety of biomedical applications, such as antimicrobial, antifungal, antioxidant, anticancer, and antiparasitic properties [11,12].

Several studies have shown that coating or conjugating ZnO-NPs could improve/enhance their biological functions, biocompatibility, and feasibility for the formulation for in vivo use. ZnO-NPs were coated with curcumin, cinnamaldehyde, thymol, tannic acid, salicylic acid, and others [13–16]. The use of ZnO@Eug nanocomposites as dental sealants has been demonstrated in several studies. According to the previous studies, Zn-Eug sealer showed low toxicity in vitro and high biocompatibility in an animal model [17–19]. ZnO-NPs synthesized by green materials could be a suitable alternative to antiparasitic drugs. Studies have shown that combining ZnO NPs and phytochemicals can remarkably impact microbial infections, including *Toxoplasma*, a prevalent concern. Considering that Eug and ZnO-NPs have potential biological properties and no such study has been conducted so far, thus the present study focused on nanoformulation based on ZnO-NPs coated with Eug for the first time to eliminate *T. gondii* in mice and ex-vivo samples.

2. Materials and methods

2.1. Chemicals and cell line preparation

Eugenol and 4-(2-pyridylazo) resorcinol were purchased from Sigma (St. Louis, MO, USA). Polyvinyl alcohol (PVA), dimethyl sulfoxide (DMSO), Zn $(NO_3)_2$, Tween 80, and sodium hydroxide (NaOH) were procured from Merck company (Merck, Germany). Vero cells were obtained from the Pasteur Institute in Tehran, Iran.

2.2. Animal ethics and in vivo studies

In vivo experiments were performed on Balb/c mice aged 8–10-week with 20–25 g weight. All protocols were considered based on the animal ethics standards with permission of ethics committees of the research deputy of Lorestan University of medical sciences.

2.3. ZnO-NPs preparation

ZnO-NPs were prepared by a chemical method using NaOH and PVA as reducing and stabilizing agents. For this purpose, 2.6 g of Zn $(NO_3)_2{\cdot}4H_2O$ was prepared in 100 mL of PVA solution (0.01% in deionized water) and then 0.5 M of NaOH was added dropwise while shaking on a magnetic stirrer. After 4 h, a white suspension appeared in the reaction solution, confirming the formation of ZnO-NPs. The solution was centrifuged at 10,000 rpm for 15 min to recover the precipitate. The white precipitate was rinsed three times with distilled water to remove any remaining impurities and the final product was dried at 65 °C in an oven for 24 h [20].

2.4. ZnO@Eug suspension formation

In a beaker, 40 mL of ethanolic solution (50%) of PVA (1.2%), Eug (0.5%) and Tween 80 (0.1%) was placed in a magnetic stirrer at 50 °C. After that, 0.6 g of ZnO-NPs was dissolved in 10 mL of deionized water and dropwise added to the sample suspension. Ultrasonication was conducted to prepare a homogenous suspension as seen by visual observation. The beaker was transferred to an ultrasonic bath (Q500 sonicator, Qsonica, USA) and sonicated at 100 W, 20 kHz in a 5 s on/off pulse mode h at 60 °C for 1. Finally, the prepared nanosuspension was kept at room temperature for the next studies. Fig. 1 illustrates a summary of ZnO@Eug formation by

ZnO-NPs and Eug ethanolic emulsion [21].

2.5. Characterization of ZnO-@Eug

Morphological properties were examined using FESEM electron microscope (TESCAN MIRA3, Oxford, Czech Republic) equipped with FEG-EDAX instrument at 30 kV. For this, 100 mg of ZnO-NPs or ZnO@Eug Nanocomposites was dispersed on a sticky stub and coated with a gold layer to reduce its charging effects. The images were taken at 200 KX with a view field of 4.97 μm. Elemental analyses of the samples were conducted using an energy-dispersive X-ray (EDX) detector. The functional groups involved in nanostructures were studied by an FTIR spectrometer (Bruker IFS 66/s, Bruker Optics, Billerica, MA) at 400-4000 cm^{-1} with a resolution of 1 cm^{-1}. The nanostructures' particle size distribution and zeta potential were determined using dynamic light scattering (DLS) on a Zetasizer Nano ZS90 system (Malvern, U.K.).

2.6. Release kinetics of eug and ZnO-NPs

The release of Eug and zinc from ZnO@Eug NSus was monitored using a dialysis membrane in phosphate buffer saline (PBS) at room temperature. The dialysis membrane (Sigma, 12 KDa MWCO) was loaded with 5 mL of ZnO@Eug NSus, sealed by clamps and placed into a beaker containing 50 mL of PBS. The beaker was then placed on a magnetic stirrer for 120 min. In 15 min regular intervals, 5 mL of PBS was removed to analyze Eug and Zn contents. The released Eug was quantified at 280 nm using a UV–Vis spectrophotometer (Jenway 6705 UV/Vis) and Zn content in PBS was determined using the Atomic absorption spectroscopy (AAS) on PerkinElmer AAnalyst 200 (Mundelein, Illinois USA) [22].

2.7. Parasite preparation

Fresh active tachyzoites of *T. gondii*, RH strain, were harvested from the intraperitoneal cavity of infected BALB/c mice by a sterile syringe. After harvesting, tachyzoites were washed with sterile normal saline and counted by hemocytometer slide after staining with trypan blue dye. Those tachyzoites samples with up to 90% viability were considered for experimental use.

2.8. Cytotoxicity assay of the formulations

Cell toxicity of all formulations, including ZnO@Eug, ZnO-NPs and Eug, was assessed using the MTT method on the Vero cell line. Briefly, 10^5 cells per well were seeded in a 96-well plate containing 100 μl Dulbecco's Modified Eagle Medium (DMEM) supplemented with 10% FBS. Afterward, the cells were treated with 0–500 μg/mL of ZnO@Eug, ZnO-NPs, and Eug and incubated in 5% CO_2 under 95% humidity at 37 °C for 48 h. An untreated well was considered as the negative control. The culture medium was then removed, and 10 μl of MTT reagent solution (15%) was added to each well and incubated at 37 °C in 5% CO_2 for 4 h. The produced formazan was dissolved by adding DMSO (200 μl/well), maintained at 37 °C for 10 min, and then the absorbance of the solution was measured at 570 nm using an ELISA plate reader [1]. Cytotoxicity efficiency was calculated by the following equation:

$$\text{Cell cytotoxicity } (\%) = \frac{Ac - At}{Ac} \times 100$$

where, Ac and at are the absorbance of the control and treated samples, respectively.

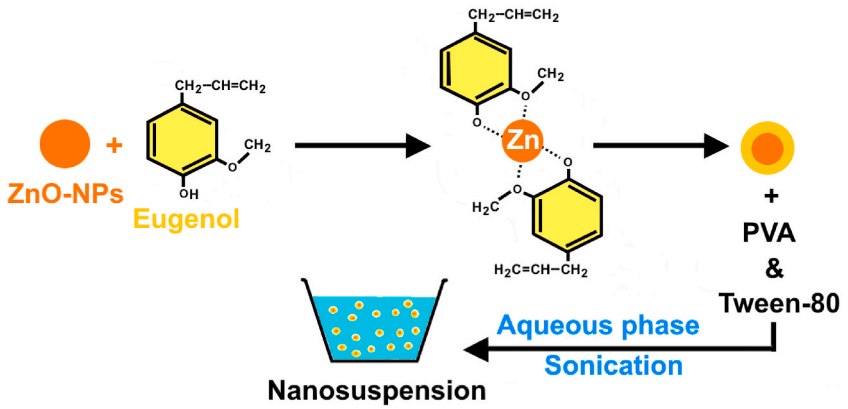

Fig. 1. Diagram of formation of ZnO-@Eug Nanosuspension.

2.9. Intracellular anti-Toxoplamsa assay

Anti-*Toxoplasma* activity of ZnO@Eug, ZnO-NPs, Eug, and spiramycin (positive control) were studied in the tachyzoites-infected Vero cells. As aforementioned, Vero cells were cultured in a 96-well plate until reaching 75% confluency. Afterward, 10^5 viable tachyzoites were added to each well to infect the cells. After 24 h incubation, cell-tachyzoite infection was monitored by a reverse light microscope. Anti-infectivity of the formulations against the infected cells was studied by treating them with sub-IC_{50} ($\sim 2/3$ IC_{50}), including ZnO@Eug, ZnO-NPs, Eug, and spiramycin. After treatment, the culture cell plate was incubated at 37 °C for 48 h. Finally, cell viability was determined based on MTT assay, and the therapeutic efficacy was calculated according to the following equation [1]:

$$\text{Therapeutic efficacy } (\%) = \frac{\text{At} - \text{Au}}{\text{At}} \times 100$$

where, A_t and A_u are the absorbance intensity of the treated and untreated infected cells, respectively.

2.10. In vitro anti-Toxoplasma activity

All formulations were studied for anti-*Toxoplasma* activity compared with ZnO@Eug and spiramycin. Similar to the previous experiment, 10^5 tachyzoites were added to each well in a 96-well plate containing Dulbecco's Modified Eagle Medium (DMEM) supplemented with 10% FBS. All treatments were performed based on 2-fold serial dilutions of ZnO-NPs (100 μg/mL), Eug (100 μg/mL), ZnO@Eug (200 μg/mL) and spiramycin (50 μg/mL). After 2 h incubation, the mortality of tachyzoites was determined by trypan-blue staining on a hemocytometer slide under a light microscope. Mortality percent was calculated as follows [1]:

$$\text{Mortality } (\%) = \frac{\text{Number of treated tachyzoites}}{\text{Number of untreated tachyzoites}} \times 100$$

2.11. In vivo anti-Toxoplasma assay

2.11.1. Animal infection and survival study

The animal experiment was performed to study the therapeutic potential of all formulations. For this, 60 male BALB/c mice 2–3 months old with 20–25 g weight were divided into 6 groups (n=10). One group was considered as uninfected control. Five groups were intraperitoneally infected with 100 μl sterile PBS containing 3000 active tachyzoites of *the T. gondii* RH strain. Each group was intraperitoneally treated with one formulation, including ZnO-NPs, ZnO@Eug, Eug and spiramycin with sub-MIC dose, except the spiramycin group administered orally and the positive control received no treatment. Another group included untreated-uninfected mice were considered as normal control. The experiment was carried out following the Ethics and Animal Care Committee protocol, and the mice were raised under standard conditions. After 14 days of follow-up, the survival rate was calculated according to the following formula [1]:

$$\text{Survival rate } (\%) = \frac{\text{Number of live mice at the 10th day}}{\text{Number of living mice at first day}} \times 100$$

2.11.2. Monitoring of tachyzoites in tissues

As described previously, we infected 30 mice with tachyzoites and divided them into 6 groups to measure tachyzoite persistence in tissues. All formulations were then administered to the mice and sacrificed on the fifth day. Tissue samples, including the liver and spleen, were removed. Also, peritoneal fluid was harvested to count its tachyzoites content. Brain samples were taken for the molecular studies described in the next section. To detect tachyzoites, tissue samples were smeared on microscope slides and stained using Giemsa solution (5%). Dead and live tachyzoites were enumerated in terms of the mean parasites on the 5 different fields under the light microscope [1].

2.11.3. Molecular detection of toxoplasma

T. gondii in the brain of infected mice was studied using PCR assay. For this, DNA was extracted from the brain tissue with Wizol DNA extraction Kit (Wizbiosolutions Inc., South Korea) according to the manufacturer's protocol. *T. gondii* DNA was detected by amplifying a 200 bp amplicon of the B1 gene using one pair primer, including OutF:5′-GGAACTGCATCCGTTCATGAG-3′ and OutR:5′-TCTTTAAAGCGTTCGTGGTC-3′. Gene B1 was amplified using the following protocol: 10 min at 95 °C, 35 cycles of 60 s at 94 °C, 60 s at 50 °C (first step) or 54 °C (second step), 60 s at 72 °C, and a final extension of 10 min at 72 °C. After that, PCR products were electrophoresed on 1% agarose gel, stained using Safe stain and visualized in the UV gel documentation system [23].

2.12. Statistical analyses

Statistical analyses were performed based on at least triplicates and differences between groups were determined by one-tail ANOVA with significant distances of p-value< 0.05.

3. Results and discussion

3.1. Physicochemical studies of ZnO@Eug

3.1.1. SEM and EDX analyses

EDX and SEM were used to demonstrate the nanostructure of ZnO-NPs embedded with and without Eug emulsion. The SEM image of PVA-ZnO-NPs showed an interaction with water-soluble polymers (PVA), resulting in randomly packed shapes with a spherical appearance (Fig. 2A). According to Fig. 2B and D of EDX patterns, when Eug was incorporated with ZnO-NPs, organic elements such as carbon significantly increased. Moreover, the agglomerated morphology of ZnO@Eug nanocomposites can be attributed to the interaction of polymer chains surrounding ZnO-NPs [24,25]. As seen in Fig. 2C, ZnO@Eug was formed by incorporating the porous structure of ZnO-PVA with emulsified Eug phase. ZnO-PVA nanostructures and ZnO@Eug nanocomposites exhibited different abundances of elemental peaks in EDX patterns.

3.1.2. Particles size and surface charge analyses

Nanodrugs are often evaluated for their stability and efficacy based on their particle size distribution in an aqueous phase. Fig. 3A and B illustrate the particle size distribution of ZnO-NPs and ZnO@Eug nanocomposites in aqueous media. According to the measurements, ZnO-NPs showed a Z-average size of 96.5 nm, while ZnO@Eug nanosuspension displayed an average size of 109.6 nm. As reported in the studies, the nanocomposites swell in aqueous solutions and their hydrodynamic diameters increase significantly [19,25,26]. The Z-average obtained by DLS in aqueous solutions is typically higher than those obtained by XRD, SEM, and TEM. This means capping molecules can affect the hydrodynamic diameter of ZnO@Eug nanosuspension [25]. The ZnO@Eug nanosuspension had a greater hydrodynamic diameter than ZnO-NPs, possibly due to the formation of lipophilic granules suspended in the aqueous phase [24]. On the other hand, increasing the density of ZnO-NPs due to interacting with Eug might enhance their dispersity and uniformity [27,28]. ZnO-NPs showed a ZP of −15 mV, while ZnO@Eug nanosuspension showed a value of −22 mV after incorporating Eug (Fig. 3C and D). As mentioned earlier, nanoparticles are usually electrostatically stabilized by a ZP above 30 mV or below −30 mV (28).

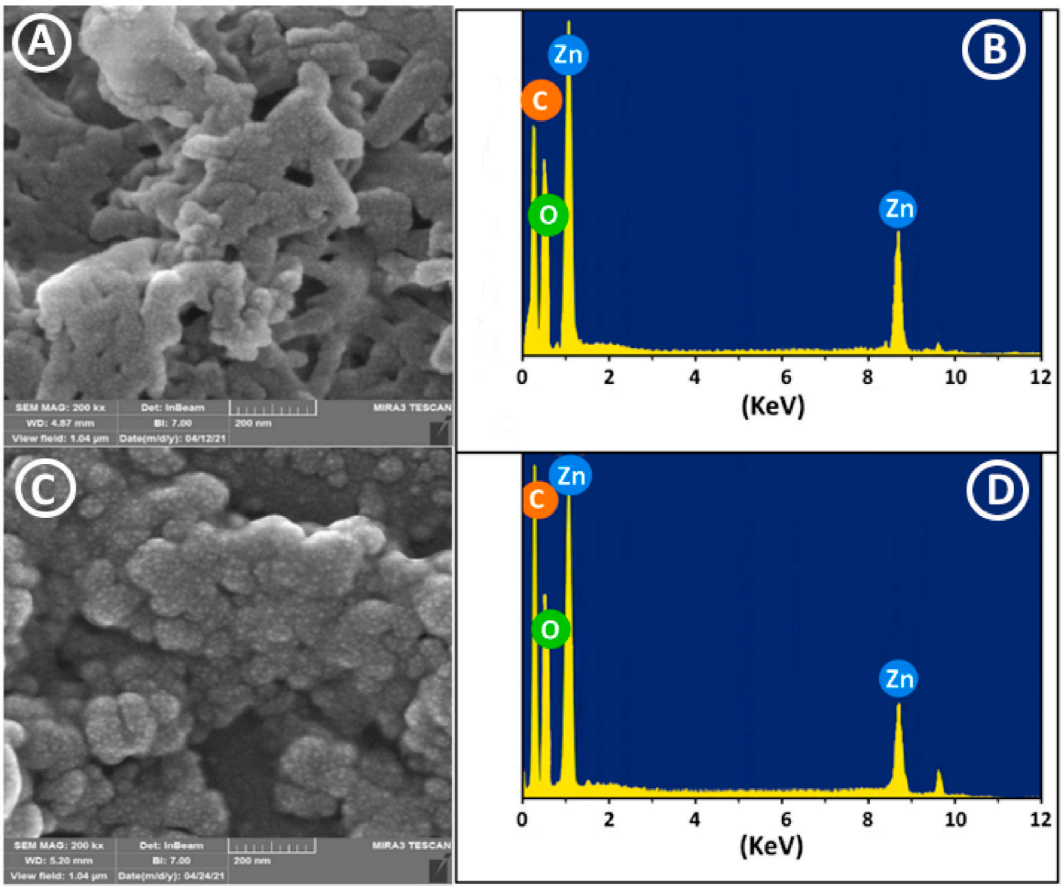

Fig. 2. SEM images and correspondence EDX of ZnO-NPs and ZnO@Eug nanocomposites. Fig. 2A and C shows the surrounding of ZnO-NPs with Eug as the porous structure of ZnO-NPs transforms into a smooth surface. Fig. 2B and D shows that organic elements such as carbon were significantly increased in ZnO@Eug nanocomposites.

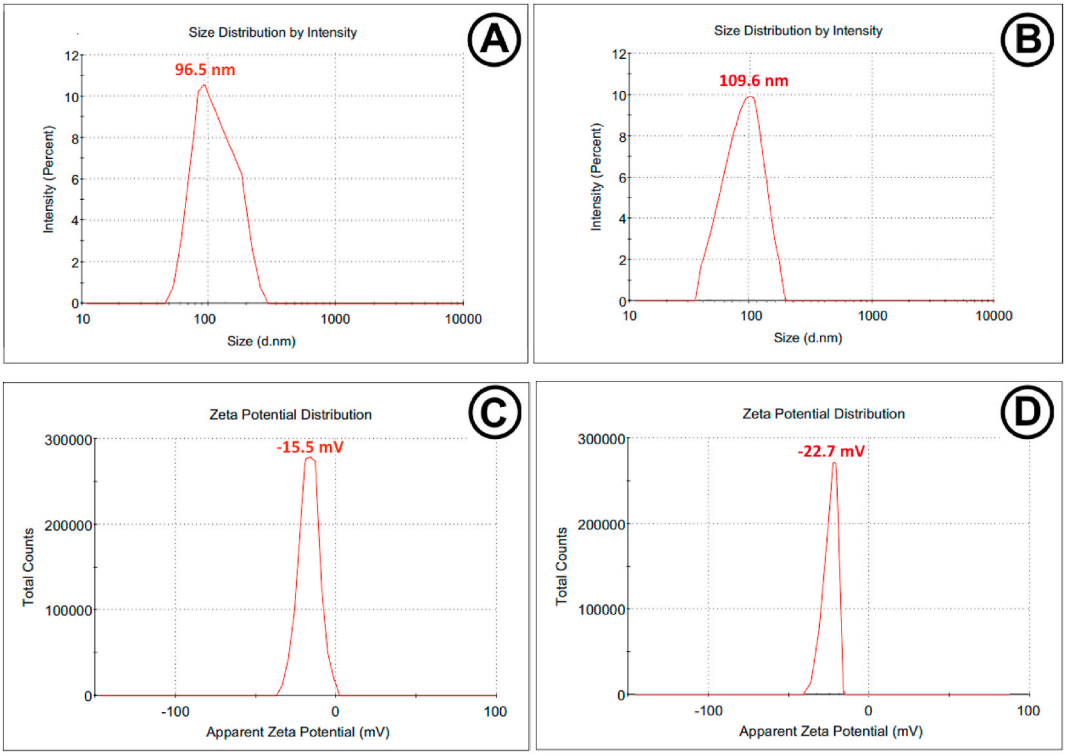

Fig. 3. Particle size distribution (DLS) and zeta potential (surface charge) of (A) and (C) for PVA-ZnO-NPs and (B) and (D) for ZnO@Eug nanosuspension in an aqueous phase.

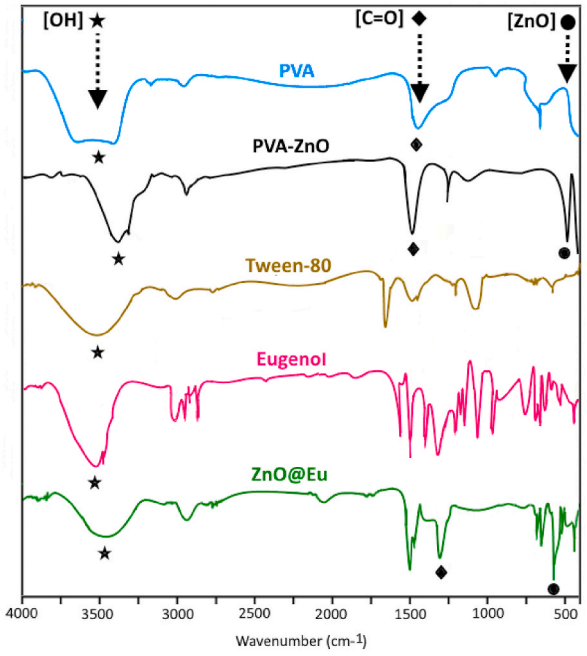

Fig. 4. Fourier transform infrared spectroscopy (FTIR) spectra of all chemicals involved in forming ZnO@Eug nanocomposites. Specific peaks are labeled as asterisks, squares, and circles.

Several studies have demonstrated that the surface charge of a material is a significant factor in its stability and catalytic capacity [29]. Further, metal NPs exhibit varying ZP values depending on their surroundings [30]. Rivera-Rangel et al. reported that biogenic synthesis increases negatively charged metal NPs and stabilizes them, preventing aggregates and agglomerations [15]. In our study, Eug acts as a coating or capping agent for ZnO-NPs, thereby altering their surface charge and increasing their anti-parasitic properties.

3.1.3. FTIR analysis

The functional interactions between PVA, Eug, and ZnO-NPs were assessed using FTIR analysis. FTIR spectra were obtained over 400 to 4000 cm^{-1} for all reactant molecules forming the ZnO@Eug nanocomposites. As seen in Fig. 4, which presents all spectral patterns, the molecules displayed a broad absorption band at 3300-3700 cm^{-1}, related to the stretching vibrations of the *O*–H bands [15,27]. A stretching bond is formed at 1469.7 cm^{-1} due to chemical interactions between Zn and the carbonyl group of PVA. According to these interpretations, the formation and stabilization of ZnO-NPs occurred by Intra/intermolecular electrostatic interactions between Zn and PVA molecules [31]. ZnO@Eug nanocomposite presented a noticeable change with an appearance of a bending peak at 498.1 cm^{-1}, indicating the presence of Zn ions [32,33].

3.1.4. Release kinetics of eug and ZnO-NPs

The release rate of ZnO-NPs and Eug from ZnO@Eu nanocomposite was measured at time intervals of 15 min for 2 h. The highest release (~60%) of ZnO-NPs and Eug occurred during the first 45 min and then stabilized (Fig. 5A). Multiple factors can affect the release rate of ZnO-NPs and Eug, including electrochemical conditions, hydrophobic interactions, and composite stability at different pH, temperature, and osmolarity [34–37]. Additionally, the morphology and size of nanocomposites play a critical role in degradability, resulting in a leakage of compounds [38]. However, some literature claimed that degradation by swelling might directly affect the kinetics of drug release in nanocomposites [39,40]. The results of our study indicated that the ZnO@Eug nanocomposites could provide sustained release of ZnO-NPs and Eug. Therefore, ZnO@Eug nanocomposites can improve the antiparasitic effect and reduce the cytotoxicity on host cells by exhibiting sustained release.

3.2. Cytotoxicity assay of the formulations

The cytotoxicity effect of three formulations, ZnO-NPs, Eug and ZnO@Eug NSus, was examined against the Vero cells using the MTT assay method. The results indicated that the cytotoxicity of three formulations followed by dose-dependent status so that the cell viability decreased with increased compound concentration. As shown in Fig. 5A, the IC_{50} values for treatments of ZnO-NPs, Eug and ZnO@Eug were 71.85, 22.39, and 47.81 μg/mL, respectively.

Cell viability was measured in different treatments, in which ZnO-NPs with IC_{50} values of 70.85 μg/mL showed the least cytotoxicity (Fig. 5B). The decrease in IC_{50} of ZnO@Eug (47.81 μg/mL) suggests that ZnO@Eug had greater penetration into parasites due to increased hydrophobicity [41,42]. There was substantial evidence that capping and coating agents affected metal nanoparticles' physiological properties and biological activities. Accordingly, Javed et al. found that polyethylene glycol (PEG) and polyvinylpyrrolidone (PVP) capped ZnO-NPs exhibited more antimicrobial activity [13]. According to El-Kattan et al., curcumin-capped ZnO-NPs effectively against a broad range of clinically pathogenic bacteria. The occurrence can be attributed to the increased hydrophobicity of ZnO-NPs, causing strong penetration into the bacteria [43]. The role of bioactive materials as capping agents in modulating the cytotoxicity of ZnO-NPs has frequently been demonstrated [44,45]. Consequently, Eug modulates the side effects of ZnO-NPs, thereby improving their therapeutic efficacy.

3.3. Intracellular anti-Toxoplamsa assay

ZnO@Eug, ZnO-NPs, and Eug were tested on Vero cells for their effectiveness against intracellular infection with *T. gondii*. For this,

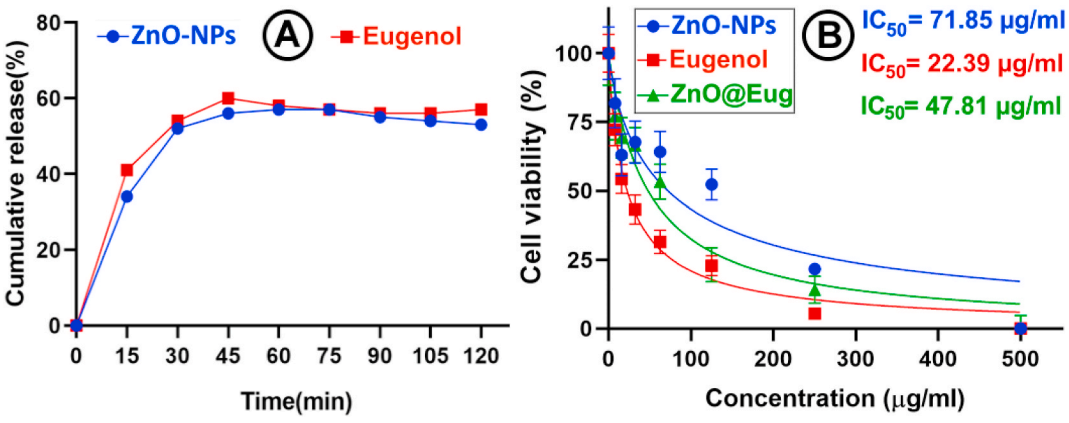

Fig. 5. (A) Release kinetics of ZnO-NPs and Eug from Zno@Eug nanocomposites and (B) cytotoxicity effects of three formulations on Vero cell line.

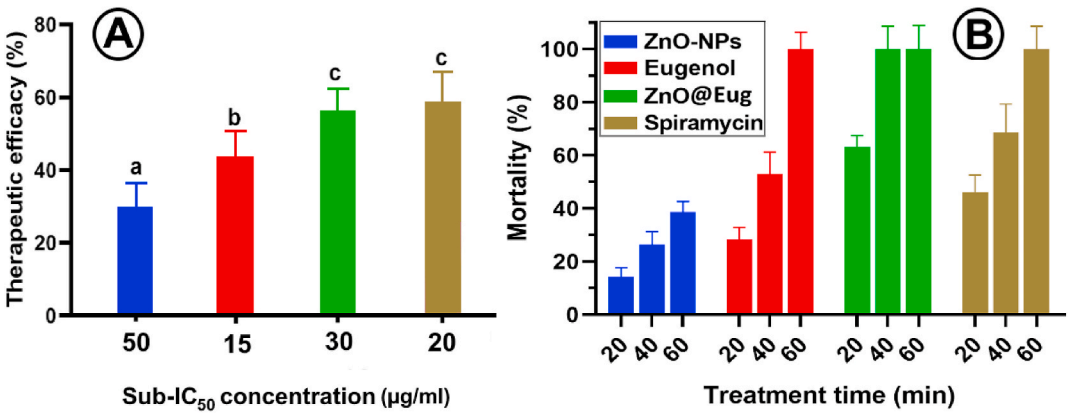

Fig. 6. (**A**) Therapeutic efficacy (%) of the formulations on the infected cell lines (**B**) Anti-*Toxoplasma* activity of formulations against infection of *T. gondii* with 20, 40, and 60-min exposure.

the Sub-IC_{50} values of ZnO@Eug (IC_{50} = 30 µg/mL), ZnO-NPs (IC_{50} = 50 µg/mL, Eugenol (IC_{50} = 15 µg/mL) and spiramycin (IC_{50} = 20 µg/mL) were used for intracellular anti-*Toxoplasma* activity assessments (Fig. 6A and B).

The highest anti-*Toxoplasma* activity was obtained for ZnO@Eug Nsus with therapeutic efficacy of 56.3%, while there was no significant difference with spiramycin (58.9%) (Positive-control). Although a significant difference in anti-*Toxoplasma* for ZnO-NPs treated groups were observed with others, as it turned out, sustained release of the ZnO-NPs significantly synergized its anti-*Toxoplasma* efficiency [46].

3.4. In vitro anti-Toxoplasma activity

The viability of *T. gondii* Tachyzoites obtained from infected mice was examined in vitro using different formulations at sub-IC_{50} concentrations. The highest anti-*Toxoplasma* activity occurred in those groups exposed to ZnO@Eug, Eugenol, and spiramycin for 60 min. Among all treatments, only ZnO-NPs treated groups tended to mortality at 60 min, with a rate of 38.7%.

Since all formulations were directly in contact with tachyzoites, they showed no statistically significant differences in mortality efficacy. ZnO-NPs treated groups showed the lowest anti-*Toxoplasma* activity, which may be attributed to their low aqueous solubility. Accordingly, several studies have demonstrated the strong antiparasite effects of plant essential oils, particularly against *Toxoplasma*. Plant metabolites such as lactones, polyphenols, and terpenoids were shown to be potent antiparasite agents in many studies.

In this regard, Yao et al. showed that *Origanum vulgare* essential oil has strong anti-*Toxoplasma* properties [47]. Another study showed that Eug and cinnamaldehyde could drastically inhibit *Leishmania* promastigotes in vitro [48]. Saadatmand et al. examined the effects of biogenic ZnO-NPs against *T. gondii* in mice. They showed no *T. gondii* was found in the brain tissue after 14 days of treatment with 150 mg/kg of ZnO-NPs [12]. Al-Humaidi et al. stated that ZnO-NPs coated with carbon nanotubes could significantly increase their anti-*Toxoplasma* activity [49]. Our findings showed decoration of ZnO-NPs with Eug could significantly provide a potent formulation for killing *T. gondii* with improved host toxicity.

3.5. In vivo anti-Toxoplasma assay

The therapeutic activity of all formulations is illustrated in Fig. 7A and B. The results demonstrated that 50% of untreated infected mice died after a four-day infection, while ZnO@Eug and Eug-treated groups survived for up to 14 days. Fig. 7B illustrates cumulative survival, which showed a survival rate of up to 7 days for control and ZnO-NPs-treated groups, while the ZnO@Eug-treated group showed a survival rate of 13 days.

Additionally, counts of *Toxoplasma* were determined in the treated and untreated groups' liver, spleen, and peritoneal fluid (Table 1). Tachyzoites were found in the least number in the group treated with Eugenol and Spiramycin. Afterward, ZnO@Eug and ZnO-NPs had the lowest tachyzoite infectivity. *T. gondii* DNA from brain tissue was amplified by PCR and then electrophoresed. In Fig. 8, both ZnO@Eug and Eug groups had weak bands on gel electrophoresis, indicating low levels of DNA from tachyzoites in the brains. Several studies have confirmed that plant-derived essential oils protect vital organs such as the brain, liver, and spleen from *Toxoplasma* infection. Oliveira et al. found that estragol and thymol effectively treat *T. gondii* tachyzoites infection in pregnant mice [50].

In addition, Khamesipour et al. reported that essential oils from *Dracocephalum kotschyi* significantly increased the survival time of mice infected with *Toxoplasma* [51]. According to Teimouri et al. chitosan nanoparticles can significantly reduce *Toxoplasma* Tachyzoites counts in the brain and liver of mice [52]. Several studies have demonstrated that metal NPs incorporated with essential oils may enhance in vivo antibacterial, antifungal, antiviral, and anti-parasitic activity. Shankar et al. incorporated ZnO-NPs into PLA nanocomposites to enhance their antibacterial activity [53]. Costa et al. replaced silver NPs with a conventional therapeutic regimen (sulfadiazine + pyrimethamine) for congenital toxoplasmosis that observed a favorable outcome [54]. Here, our results demonstrate

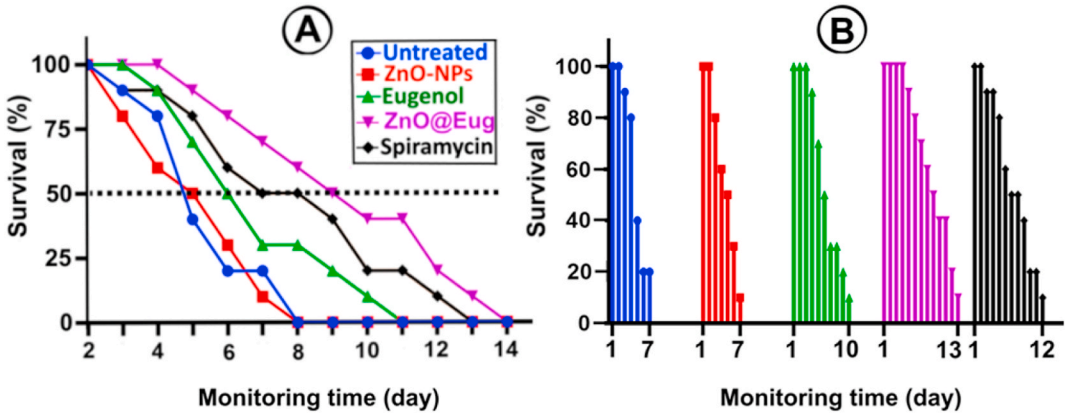

Fig. 7. Animal survival study. (A) Percentage survival of treated groups for 14 days and (B) survival monitoring based on last stage death for all groups on treatment days.

Table 1
Toxoplasma tachyzoite infection in spleen, liver, and peritoneal tissues treated by the formulations.

Group	Mean No. Of tachyzoites in tissues (reduction percentage after treatment)		
	Liver	Spleen	peritoneum
Infected[a]	10.24 ± 3.21 (0%)	6.41 (0%)	117.49 (0%)
ZnO-NPs	7.54 (25.61%)	5.34 (16.69%)	102.24 (12.97%)
ZnO@Eu	5.10 (50.19%)	4.38 (31.66%)	42.71 (63.64%)
Eugenol	3.65 (64.35%)	2.71 57.72%)	26.11 (77.77%)
Spiramycin	4.23 (58.69%)	2.36 (63.18%)	37.09 (68.43%)

[a] *T. gondii* infected mice without any treatment (positive control).

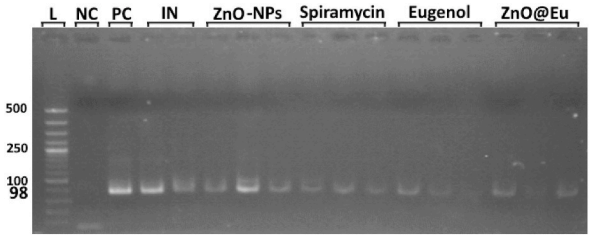

Fig. 8. Detection of *Toxoplasma* in the brain tissues of all treated groups. Based on the electrophoresis of the PCR products, all wells containing the molecular weight ladder (L), negative control (NC), positive control (PC), infected-untreated (IN) and other treated groups can be seen in the gel.

that ZnO-NPs coated with Eug provide an optimistic therapeutic formulation for influencing all organs and targeting *Toxoplasma* infections.

4. Conclusions

This study presents a formulation based on ZnO-NPs coated with Eug to improve its stability and anti-*Toxoplasma* activity. The ZnO-NPs@Eug Nsus could release sustainably and have low toxicity, allowing them to be used synergistically for treating experimental toxoplasmosis in animal models. The findings of this study represent the development of a new pharmaceutical formulation combining NPs with natural metabolites to inhibit *Toxoplasma* infection. Thus, the proposed therapeutic approach against *Toxoplasma* can be achieved by utilizing Eug and ZnO-NPs as highly effective bioactive provided details concerning their toxicity, bioavailability and possible side effects are clarified.

Author contribution statement

Kourosh Cheraghipoura: Conceived and designed the experiments; Analyzed and interpreted the data. Hossein Mahmoudvand: Conceived and designed the experiments; Wrote the paper. Kobra Moradpoura, Masoomeh Zivdaria, Marjan Beiranvand: Performed the experiments; Contributed reagents, materials, analysis tools or data. Amal Khudair Khalaf: Analyzed and interpreted the data.

Pegah Shakib: Contributed reagents, materials, analysis tools or data. Abdolrazagh Marzban: Performed the experiments; Analyzed and interpreted the data; Contributed reagents, materials, analysis tools or data; Wrote the paper.

Funding

None.

Availability of data and materials

All the data during of this study are included in the article.

Ethics approval and consent to participate

The protocols of this investigations are in line with the approvals of the Guide for the Care and Use of Laboratory Animals of the National Institutes of Health; which was agreed by the Ethics Committee of the Lorestan University of Medical Sciences, Iran (IR.LUMS.REC.1398.290). This study was carried out in compliance with the ARRIVE guidelines (https://arriveguidelines.org/).

Consent for publication

Not applicable.

Declaration of competing interest

The authors declare that they have no known competing financial interests or personal relationships that could have appeared to influence the work reported in this paper.

Acknowledgements

We would like to thank the staff of Razi Herbal Medicines Research Center, Khorramabad, Iran.

References

[1] K. Cheraghipour, M. Zivdari, M. Beiranvand, P. Shakib, F. Kheirandish, M.Z. Pour, et al., Encapsulation of Nepeta cataria essential oils in a chitosan nanocomposite with lethality potential against Toxoplasma gondii, Emergent Materials (2022) 1–11.
[2] N.C. Smith, C. Goulart, J.A. Hayward, A. Kupz, C.M. Miller, G. van Dooren, Control of human toxoplasmosis, Int. J. Parasitol. 51 (2–3) (2021) 95–121.
[3] D. Daher, A. Shaghlil, E. Sobh, M. Hamie, M.E. Hassan, M.B. Moumneh, et al., Comprehensive overview of Toxoplasma gondii-induced and associated diseases, Pathogens 10 (11) (2021) 1351.
[4] M. Ahmed, A. Sood, , Gupta JJEJoO, Gynecology, R. Biology, Toxoplasmosis in pregnancy, Eur. J. Obstet. Gynecol. Reprod. Biol. 255 (2020) 44–50.
[5] K. Bhagat, N. Kumar, H. Kaur Gulati, A. Sharma, A. Kaur, J.V. Singh, et al., Dihydrofolate reductase inhibitors: patent landscape and phases of clinical development (2001–2021), Expert Opin. Ther. Pat. 32 (10) (2022) 1079–1095.
[6] J.P.F. Felix, R.P.C. Lira, A.T. Grupenmacher, H.L.G. de Assis Filho, A.B. Cosimo, M.A. Nascimento, et al., Long-term results of trimethoprim-sulfamethoxazole versus placebo to reduce the risk of recurrent Toxoplasma gondii retinochoroiditis, Am. J. Ophthalmol. 213 (2020) 195–202.
[7] M. Sharif, S. Sarvi, A.S. Pagheh, S. Asfaram, M.T. Rahimi, S. Mehrzadi, et al., The efficacy of herbal medicines against Toxoplasma gondii during the last 3 decades: a systematic review, Can. J. Physiol. Pharmacol. 94 (12) (2016) 1237–1248.
[8] T. Anand, M. Anbukkarasi, P.A. Thomas, Technology Geraldine PjjoDDS, A comparison between plain eugenol and eugenol-loaded chitosan nanoparticles for prevention of in vitro selenite-induced cataractogenesis, J. Drug Deliv. Sci. Technol. 65 (2021), 102696.
[9] M. Ulanowska, Olas BJIJoMS, Biological Properties and prospects for the application of eugenol—a review, Int. J. Mol. Sci. 22 (7) (2021) 3671.
[10] A. Abdou, A. Elmakssoudi, A. El Amrani, J. JamalEddine, M.J.M.C.R. Dakir, Recent advances in chemical reactivity and biological activities of eugenol derivatives, Trends in Sciences 30 (5) (2021) 1011–1030.
[11] G. Bondareva, G. Stadnyuk, T. Grebennikova, M. Shashlova, Donina MJSRiP, Antimicrobial properties of some zinc compounds, Sys. Rev. Pharm. 11 (12) (2020).
[12] M. Saadatmand, G.R.L. Al-Awsi, A.D. Alanazi, A. Sepahvand, M. Shakibaie, S. Shojaee, et al., Green synthesis of zinc nanoparticles using Lavandula angustifolia Vera. Extract by microwave method and its prophylactic effects on Toxoplasma gondii infection, Saudi J. Biol. Sci. 28 (11) (2021) 6454–6460.
[13] R. Javed, M. Usman, S. Tabassum, M.J.A.S.S. Zia, Effect of capping agents: structural, optical and biological properties of ZnO nanoparticles, Appl. Surf. Sci. 386 (2016) 319–326.
[14] A.E. Albalawi, S. Abdel-Shafy, A. Khudair Khalaf, A.D. Alanazi, P. Baharvand, K. Ebrahimi, H. Mahmoudvand, Therapeutic potential of green synthesized copper nanoparticles alone or combined with meglumine antimoniate (glucantime®) in cutaneous leishmaniasis, Nanomaterials 11 (4) (2021) 891.
[15] R.D. Rivera-Rangel, M.P. González-Muñoz, M. Avila-Rodriguez, T.A. Razo-Lazcano, C.J.C. Solans, S.A. Physicochemical, et al., Green synthesis of silver nanoparticles in oil-in-water microemulsion and nano-emulsion using geranium leaf aqueous extract as a reducing agent, Colloids Surf. A Physicochem. Eng. Asp. 536 (2018) 60–67.
[16] J. Shin, A. Naskar, D. Ko, S. Kim, Kim K-sJIJoMS, Bioconjugated thymol-zinc oxide nanocomposite as a selective and biocompatible antibacterial agent against Staphylococcus species, Int. J. Mol. Sci. 23 (12) (2022) 6770.
[17] M. Javidi, M. Zarei, S. Omidi, A. Ghorbani, M. Gharechahi, Rad MSJIej, Cytotoxicity of a new nano zinc-oxide eugenol sealer on murine fibroblasts, Iran. Endod. J. 10 (4) (2015) 231.
[18] H. Mahmoudvand, F. Kheirandish, M. Ghasemi Kia, A. Tavakoli Kareshk, M. Yarahmadi, Chemical composition, protoscolicidal effects and acute toxicity of Pistacia atlantica Desf. fruit extract, Nat. Prod. Res. 30 (10) (2016) 1208–1211.
[19] A. Keyhani, N. Ziaali, M. Shakibaie, A.T. Kareshk, S. Shojaee, M. Asadi-Shekaari, M. Sepahvand, H. Mahmoudvand, Biogenic selenium nanoparticles target chronic toxoplasmosis with minimal cytotoxicity in a mouse model, J. Med. Microbiol. 69 (1) (2020) 104–110.
[20] A. Devi, V. Sudan, A. Jaiswal, A. Singh, D. Shanker, B1 gene based semi nested PCR for detection of toxoplasmosis from poultry hearts, Indian J. Anim. Sci. 87 (8) (2017) 980–981.

[21] M. Mirhosseini, F.B. Firouzabadi, Antibacterial activity of zinc oxide nanoparticle suspensions on food-borne pathogens, Int. J. Dairy Technol. 66 (2) (2013) 291–295.
[22] I. Erol, Ö. Hazman, M. Aksu, Preparation of novel composites of polyvinyl alcohol containing hesperidin loaded ZnO nanoparticles and determination of their biological and thermal properties, J. Inorg. Organomet. Polym. Mater. 33 (3) (2023), 731-346.
[23] N.A. Al-Dhabi, M.J.N. Valan Arasu, Environmentally-friendly green approach for the production of zinc oxide nanoparticles and their anti-fungal, ovicidal, and larvicidal properties, Nanomaterials 8 (7) (2018) 500.
[24] H.M. Al-Kordy, S.A. Sabry, M.E. Mabrouk, Statistical optimization of experimental parameters for extracellular synthesis of zinc oxide nanoparticles by a novel haloalaliphilic Alkalibacillus sp. W7, Sci. Rep. 11 (1) (2021) 1–14.
[25] O.R. Abbasabadi, M.R. Farahpour, Tabatabaei ZgjijoBM, Accelerative effect of nanohydrogels based on chitosan/ZnO incorporated with citral to heal the infected full-thickness wounds; an experimental study, Int. J. Biol. Macromol. 217 (2022) 42–54.
[26] S. Modi, V.K. Yadav, N. Choudhary, A.M. Alswieleh, A.K. Sharma, A.K. Bhardwaj, et al., Onion peel waste mediated-green synthesis of zinc oxide nanoparticles and their phytotoxicity on mung bean and wheat plant growth, Materials 15 (7) (2022) 2393.
[27] R. Gupta, P. Malik, N. Das, Singh MJJoML, Antioxidant and physicochemical study of Psidium guajava prepared zinc oxide nanoparticles, J. Mol. Liq. 275 (2019) 749–767.
[28] S. Vorobyev, M. Likhatski, A. Romanchenko, N. Maksimov, S. Zharkov, A. Krylov, et al., Colloidal and deposited products of the interaction of tetrachloroauric acid with hydrogen selenide and hydrogen sulfide in aqueous solutions, Minerals 8 (11) (2018) 492.
[29] I.A. Mir, K. Rawat, H.J.C. Bohidar, S.A. Physicochemical, E. Aspects, Interaction of plasma proteins with ZnSe and ZnSe@ ZnS core-shell quantum dots, Colloids Surf. A Physicochem. Eng. Asp. 520 (2017) 131–137.
[30] J.S. Al-Brahim, Mohammed Aejsjobs, Antioxidant, cytotoxic and antibacterial potentials of biosynthesized silver nanoparticles using bee's honey from two different floral sources in Saudi Arabia, Saudi J. Biol. Sci. 27 (1) (2020) 363–373.
[31] S.A. Awad, Khalaf EMJJoTCM, Evaluation of the photostabilizing efficiency of polyvinyl alcohol–zinc chloride composites, J. Thermoplast. Compos. Mater. 33 (1) (2020) 69–84.
[32] R. Kandulna, R.J.P.B. Choudhary, Concentration-dependent behaviors of ZnO-reinforced PVA–ZnO nanocomposites as electron transport materials for OLED application, Polym. Bull. 75 (7) (2018) 3089–3107.
[33] B. Liu, Y. You, H. Zhang, H. Wu, J. Jin, HJRa Liu, Synthesis of ZnO nano-powders via a novel PVA-assisted freeze-drying process, RSC Adv. 6 (111) (2016) 110349–110355.
[34] T.N. Barradas, de Holanda e Silva KGJECL, Nanoemulsions of essential oils to improve solubility, stability and permeability: a review, Environ. Chem. Lett. 19 (2) (2021) 1153–1171.
[35] L.O. Cinteza, C. Scomoroscenco, S.N. Voicu, C.L. Nistor, S.G. Nitu, B. Trica, et al., Chitosan-stabilized Ag nanoparticles with superior biocompatibility and their synergistic antibacterial effect in mixtures with essential oils, Nanomaterials 8 (10) (2018) 826.
[36] T.F. Moghadam, S. Azizian, Wettig SJPCCP, Synergistic behaviour of ZnO nanoparticles and gemini surfactants on the dynamic and equilibrium oil/water interfacial tension, Phys. Chem. Chem. Phys. 17 (11) (2015) 7122–7129.
[37] I.D. Rupenthal, P. Agarwal, B. Uy, J. Kim, A.A. Cunningham, A. Seyfoddin, et al., Preparation and characterisation of a cyclodextrin-complexed mānuka honey microemulsion for eyelid application, Pharmaceutics 14 (7) (2022) 1493.
[38] M. Yadollahi, S. Farhoudian, S. Barkhordari, I. Gholamali, H. Farhadnejad, Motasadizadeh Hjijobm, Facile synthesis of chitosan/ZnO bio-nanocomposite hydrogel beads as drug delivery systems, Int. J. Biol. Macromol. 82 (2016) 273–278.
[39] S.K. Pt, V.-K. Lakshmanan, M. Raj, R. Biswas, T. Hiroshi, S.V. Nair, et al., Evaluation of wound healing potential of β-chitin hydrogel/nano zinc oxide composite bandage, Pharmaceut. Res. 30 (2) (2013) 523–537.
[40] R. Rakhshaei, H. Namazi, H. Hamishehkar, H.S. Kafil, Salehi RjjoAPS, In situ synthesized chitosan–gelatin/ZnO nanocomposite scaffold with drug delivery properties: higher antibacterial and lower cytotoxicity effects, J. Appl. Polym. Sci. 136 (22) (2019), 47590.
[41] S. Savir, J.W.K. Liew, I. Vythilingam, Y.A.L. Lim, C.H. Tan, K.S. Sim, et al., Nickel (II) complexes with polyhydroxybenzaldehyde and O, N, S tridentate thiosemicarbazone ligands: synthesis, cytotoxicity, antimalarial activity, and molecular docking studies, J. Mol. Struct. 1242 (2021), 130815.
[42] N. Shinjyo, H. Nakayama, K. Ishimaru, K. Hikosaka, F. Mi-Ichi, K. Norose, et al., Hypericum erectum alcoholic extract inhibits Toxoplasma growth and Entamoeba encystation: an exploratory study on the anti-protozoan potential, J. Nat. Med. 74 (1) (2020) 294–305.
[43] N. El-Kattan, A.N. Emam, A.S. Mansour, M.A. Ibrahim, A.B. Abd El-Razik, K.A. Allam, et al., Curcumin assisted green synthesis of silver and zinc oxide nanostructures and their antibacterial activity against some clinical pathogenic multi-drug resistant bacteria, RSC Adv. 12 (28) (2022) 18022–18038.
[44] P. Basnet, T.I. Chanu, D. Samanta, SJJoP. Chatterjee, P.B. Biology, A review on bio-synthesized zinc oxide nanoparticles using plant extracts as reductants and stabilizing agents, J. Photochem. Photobiol. B Biol. 183 (2018) 201–221.
[45] H. Hozyen, E. Ibrahim, E. Khairy, SJVw El-Dek, Enhanced antibacterial activity of capped zinc oxide nanoparticles: a step towards the control of clinical bovine mastitis, Vet. World 12 (8) (2019) 1225.
[46] J. Ju, X. Chen, Y. Xie, H. Yu, Y. Guo, Y. Cheng, et al., Application of essential oil as a sustained release preparation in food packaging, Trends Food Sci. Technol. 92 (2019) 22–32.
[47] N. Yao, Q. Xu, J.-K. He, M. Pan, Z.-F. Hou, D.-D. Liu, et al., Evaluation of Origanum vulgare essential oil and its active ingredients as potential drugs for the treatment of toxoplasmosis, Front. Cell. Infect. Microbiol. (2021) 1141.
[48] U. Sharma, A.K. Sharma, A. Gupta, R. Kumar, A. Pandey, A.J.C. Pandey, et al., Pharmacological activities of cinnamaldehyde and eugenol: antioxidant, cytotoxic and anti-leishmanial studies, Cell. Mol. Biol. 63 (6) (2017) 73–78.
[49] J.Y. Al-Humaidi, M. Hagar, B.A. Bakr, B.H. Elwakil, E.A. Moneer, M.J.M. El-Khatib, Decorative multi-walled carbon nanotubes by ZnO: synthesis, characterization, and potent anti-toxoplasmosis activity, Metals 12 (8) (2022) 1246.
[50] C.B. Oliveira, Y.S. Meurer, T.L. Medeiros, A.M. Pohlit, M.V. Silva, T.W. Mineo, et al., Anti-Toxoplasma activity of estragole and thymol in murine models of congenital and noncongenital toxoplasmosis, J. Parasitol. 102 (3) (2016) 369–376.
[51] F. Khamesipour, S.M. Razavi, S.H. Hejazi, S.M.J.F.S. Ghanadian, Nutrition. In vitro and in vivo Anti-Toxoplasma activity of Dracocephalum kotschyi essential oil, Food Sci. Nutr. 9 (1) (2021) 522–531.
[52] A. Teimouri, S.J. Azami, H. Keshavarz, F. Esmaeili, R. Alimi, S.A. Mavi, et al., Anti-Toxoplasma activity of various molecular weights and concentrations of chitosan nanoparticles on tachyzoites of RH strain, Int. J. Nanomed. 13 (2018) 1341.
[53] S. Shankar, L.-F. Wang, C.E. Rhim J-Wjms, Incorporation of zinc oxide nanoparticles improved the mechanical, water vapor barrier, UV-light barrier, and antibacterial properties of PLA-based nanocomposite films, Mater. Sci. Eng. C 93 (2018) 289–298.
[54] I.N. Costa, M. Ribeiro, P. Silva Franco, R.J. da Silva, T.E. de Araújo, I.C.B. Milián, et al., Biogenic silver nanoparticles can control Toxoplasma gondii infection in both human trophoblast cells and villous explants, Front. Microbiol. 11 (2021), 623947.